Pattern Formation in a Cavity Longer than the Coherence Length of the Light in It

Tal Carmon,[1] Marin Soljačić,[2] and Mordechai Segev[1]
[1]*Physics Department, Technion–Israel Institute of Technology, Haifa 32000, Israel*
[2]*Physics Department, Massachusetts Institute of Technology, Cambridge, Massachusetts 02139*
(Received 21 December 2001; published 11 October 2002)

We study, theoretically and experimentally, the evolution of patterns in a passive nonlinear cavity that is longer than the coherence length of the light circulating in it. The patterns exhibit spatial line narrowing as the feedback is increased, resembling the line narrowing in lasers.

DOI: 10.1103/PhysRevLett.89.183902 PACS numbers: 42.65.Sf, 89.75.Kd

Pattern formation in optical cavities has been the subject of continuing interest since lasers were discovered [1–4]. Patterns naturally start from noise, from which some frequencies experience higher gain, and, through the feedback in the cavity, they stabilize and form a pattern. Such patterns appear not only in laser cavities, but also in passive cavities employing optical nonlinearities [2,4]. Pattern formation in cavities possesses several common features that make it distinct from the patterns arising [via modulation instability (MI)] during propagation in the absence of feedback [2]. First, the instability leading to pattern formation in a cavity is "global" (absolute), whereas MI without feedback arises due to a "convective" instability. Second, cavity pattern formation (including a passive cavity) has a definite threshold. In all passive cavities studied thus far patterns form only above the pattern-formation threshold. Third, a cavity gives rise to a set of resonant frequencies, and the detuning between the frequency of the light and the nearest resonant frequency critically affects the pattern. These features are universal and also appear in the temporal domain [5]. However, all resonators studied previously in the context of pattern formation are fully coherent; i.e., the beam is monochromatic, spatially coherent, and coherent with the feedback beams circulating in the resonators for many cycles. That is, the cavity round-trip time is much shorter than the coherence time of the light.

Here we explore pattern formation in a different kind of cavity: a passive ring cavity for which the coherence length of the light is much shorter than the cavity length; that is, the coherence time is much shorter than the time it takes the light to go once around the cavity. In this low-finesse cavity, the feedback beams from different cycles are mutually incoherent with one another (the relative phase among them is random). The nonlinear medium in our cavity responds much slower than the characteristic phase fluctuation time between beams from different cycles. Thus, the resonant frequencies of our cavity, as well as the relative phase between beams from different cycles, do not play any role in the pattern-formation process. The beams from different cycles interact with one another through a nonlinear index change, Δn, that is a function of the sum of their intensities but does not depend on interference cross terms. This interaction resembles cross-phase modulation [6], yet it leads to different phenomena. We find that the patterns emerging in our cavity exhibit spatial line narrowing as the feedback and/or the nonlinearity are increased, closely resembling the narrowing of the frequency linewidth in lasers [7].

Consider the system in Fig. 1(a). A plane wave enters, passes through a nonlinear medium, and circulates in the cavity. The cavity length greatly exceeds the coherence length of the laser, so interference terms between beams from different cycles fluctuate at characteristic times equal to the coherence time of the laser, t_c. The nonlinearity has a response time $\tau \gg t_c$; thus Δn is a function of the intensity I averaged over τ. The input and output faces of the nonlinear crystal are $z = 0$ and $z = L$. A fraction, ϵ^2, of I exiting the crystal is "recycled" in the cavity.

We model our cavity when the feedback is small and the pattern is of a low modulation depth (visibility), so the entire dynamics (in temporal steady state) results from the interaction between the input beam Ψ, and the feedback beam Φ that went one cycle around the cavity. Our Δn is a function of $I = \langle|\Psi + \Phi|^2\rangle = \langle|\Psi|^2\rangle + \langle|\Phi|^2\rangle$, where the time average $\langle\,\rangle$ is taken over τ. Since in MI studies, any saturable nonlinearity initially acts as a Kerr nonlinearity for the perturbation (with the nonlinear coefficient evaluated at the intensity of the input beam) [8], we take $\Delta n \propto I$ (Kerr self-focusing). The

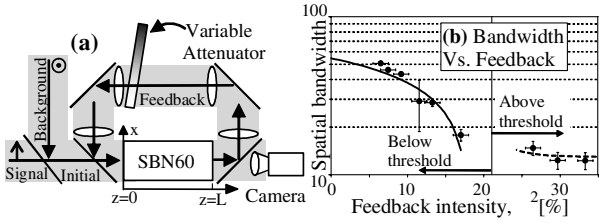

FIG. 1. (a) The incoherent resonator. (b) Bandwidth of the spatial frequency power spectrum (FWHM) as a function of feedback intensity. The experimental results are represented by crosses. The theoretical results below threshold (solid line) are based on Eq. (4) and the experimental parameters. The dashed curve above threshold is a guide to the eye.

 0031-9007/02/89(18)/183902(4)$20.00

dimensionless equations in one transverse dimension are

$$i\frac{\partial\Psi}{\partial z}+\frac{1}{2}\frac{\partial^2\Psi}{\partial x^2}+I\Psi=0; \qquad i\frac{\partial\Phi}{\partial z}+\frac{1}{2}\frac{\partial^2\Phi}{\partial x^2}+I\Phi=0. \tag{1}$$

We seek solutions of the form $\Psi(x, z, t) = \psi(x, z)\exp(i\mu z)$, $\Phi(x, z, t) = \phi(x, z)\exp(i\nu z)\exp[i\alpha(t)]$, where μ, ν are real. $\alpha(t)$ is a stochastic phase that varies much faster than τ. Taking a fraction $\epsilon(\ll 1)$ of $\Psi(x, z = L)$ from the crystal output and imaging it as feedback to the input $z = 0$ implies $\epsilon^2|\psi(x, z = L)|^2 = |\phi(x, z = 0)|^2$. Ψ starts as a plane wave ψ_0 and develops a periodic pattern due to MI. When the modulation depth of this pattern is low, ψ and ϕ each can be written as a sum of a plane wave and perturbation: $\Psi(x, z) = [\psi_0 + \psi_1(x, z)]\exp(i\mu z)$ and $\Phi(x, z) = [\phi_0 + \phi_1(x, z)]\exp(i\nu z)$, where $|\psi_1| \ll |\psi_0|$, $|\phi_1| \ll |\phi_0|$. Substituting Ψ, Φ in Eq. (1) yields $\mu = \nu = \psi_0^2$. The boundary condition gives $\phi_0 = \epsilon\psi_0$. The linearized equations for ψ_1, ϕ_1 are

$$i\frac{\partial\psi_1}{\partial z}+\frac{1}{2}\frac{\partial^2\psi_1}{\partial x^2}+\psi_0^2(\psi_1+\psi_1^*)+\phi_0(\phi_1^*+\phi_1)\psi_0=0, \tag{2}$$

$$i\frac{\partial\phi_1}{\partial z}+\frac{1}{2}\frac{\partial^2\phi_1}{\partial x^2}=0. \tag{3}$$

Here, $|\psi_0| \gg |\phi_0|$, thus ϕ is propagating mostly linearly. Without loss of generality, we seek $\phi_1(x, z) = \tilde{\phi}_a\exp[if]\cos[qx]\exp[-iq^2z/2]$, $\psi_1(x, z) = \tilde{\psi}_a\exp[if]\cos[qx]\exp[-iq^2z/2] + \psi_b\exp[i(qx + \Omega z)] + \psi_c\exp[-i(qx + \Omega^* z)]$, where $\tilde{}$ denotes the (real) modal amplitude and f is real [9]. Substitution of ψ_1 in Eq. (3) yields $\tilde{\psi}_a = -\epsilon\tilde{\phi}_a$ and $\Omega = \pm q\sqrt{(q^2/2) - (\psi_0^2)}$. For a proper Ω this pattern (with $2\pi/q$ periodicity) grows exponentially. We impose $\epsilon\Psi(x, z = L) = \Phi(x, z = 0)\exp[i\alpha(t)]$. Because $\Delta n \propto \langle I\rangle$, $\alpha(t)$ has no influence on the evolution of ψ. Using the boundary condition, the dependence of the spatial spectrum, $\hat{\psi}_1$, on q, is

$$\hat{\psi}_1(q, z = L) \propto \frac{\exp(|q|L\sqrt{\psi_0^2 - q^2/4})}{[1 - \epsilon^2\exp(|q|L\sqrt{\psi_0^2 - q^2/4})]}. \tag{4}$$

For $\epsilon = 0$ Eq. (4) converges to the known case of MI without feedback [10]. As ϵ^2 is increased, Eq. (4) yields band narrowing of the spatial spectrum, and there is a particular q at which Eq. (4) diverges, and this q dominates. This is apparent in Fig. 1(b) which shows the calculated width of $|\hat{\psi}_1|^2$ as a function of ϵ^2 (solid curve). This bandwidth narrowing means that only a single, well-defined, spatial frequency (the one with the highest growth rate) is visible at the output. Increasing ϵ^2 further causes $\hat{\psi}_1$ to diverge. This behavior is characteristic of feedback systems with gain, such as lasers [7]. The divergence indicates the presence of an oscillation threshold [11].

The intuition behind our system is subtle. First, the propagation of ϕ is mostly linear. This is manifested by Eqs. (1): ϕ and ψ cannot exchange energy because they are incoherent with one another (the temporal fluctuations in their fields are uncorrelated). ϕ_1 could grow if it could drain energy from ϕ_0. But the feedback is weak: $|\phi_0| \ll |\psi_0|$, so the MI in ϕ is much smaller than MI in ψ. Thus, MI in ϕ can be ignored. The only way ϕ_1 can evolve is due to Δn produced by ψ_1. But this happens only for large z's, where it does not have much influence on ψ, since ψ dominates its own propagation there. Nevertheless, the propagation of ϕ, albeit mostly linear, establishes a grating of period $2\pi/q$ at $z = 0$, providing a preferential "noise" for ψ. Hence, the MI in ψ does not evolve from random noise (as for $\epsilon = 0$), but instead is channeled by a particular periodic Δn induced by ϕ_1 at $z = 0$. This is embedded in the last term in Eq. (2). The contribution of ϕ_1, albeit small, is crucial. Another way to think about this is to consider the periodic Δn induced by ϕ_1 as a grating, and ψ scatters from it, changing its transverse momentum by q. Thus the q component in ψ is much bigger than it would have been if the seed grating was absent. Third, through the self-consistent process in the cavity, the q that has the largest gain is the one that grows the fastest. From this picture it is obvious that the MI growth rate is the same as for $\epsilon = 0$, but the noise gets a preferential periodicity $2\pi/q$, and this q is the one that grows fastest in MI. The larger the feedback, the stronger the seed "grating" in the input, and the stronger the amplification of that preferential grating with respect to all other gratings arising from noise. Finally, when the amount of feedback is identical to the noise amplitude in the q of highest gain, this specific q oscillates, just as in lasers. This oscillation occurs when the nonlinear gain is equal to the loss in a single cycle, as the denominator of Eq. (4) implies. When the expression in Eq. (4) diverges, the system oscillates and exhibits bandwidth narrowing [Fig. 1(b)].

In our experiment [Fig. 1(a)], we use a 488 nm Ar^+ laser beam with a 10 cm coherence length and circulate it in a 80 cm long ring cavity. The transmission spectrum of our cavity never drops more than 55% (at threshold) allowing all the bandwidth of our laser to circulate in it [12]. The nonlinear medium is an $Sr_{0.6}Ba_{0.4}Nb_2O_6$ crystal, employing the screening nonlinearity [13]. We split the laser beam into an extraordinarily polarized "signal" beam and an ordinarily polarized "background" beam [not shown in Fig. 1(a)].(The background beam is necessary for the photorefractive screening nonlinearity [13].) The ratio between the intensities of the signal and background beams is 2.1, and the applied field is 340 V/cm. The background beam is made to be highly spatially incoherent (to eliminate possible MI on it [8]), by passing it through a diffuser rotating much faster than τ. The signal and background beams are combined by a second beam splitter, expanded to a width greater than the crystal width, launched into the 5.5 mm long

crystal and propagate along its a axis. We reflect a fraction of both signal and background beams exiting the crystal, and "recycle" them in the cavity (keeping the ratio between their intensities fixed when the feedback is varied). In the feedback loop we use four lenses forming two sequential $4f$ systems, so that the intensity at the crystal output face is imaged 1:1 onto the input face (without mirror inversion). The feedback is controlled by a variable attenuator. All apertures are large enough to pass all the spatial frequencies in the system.

Starting with zero feedback, we observe emergence of low-visibility stripes (from MI), which do not have a well-defined periodicity [14]. Typical results are shown in the upper row of Fig. 2 (left) along with the spatial (Fourier) power spectrum (right). When we unblock the feedback and increase its intensity, ϵ^2, we observe obvious linewidth narrowing. We take data with ϵ^2 ranging from 0% to 33%, while keeping all other experimental parameters constant, especially the value of the nonlinearity (determined by the applied field, and the ratio between signal and background beams [13]). The linewidth narrowing is obvious (Fig. 2), as the stripes become sharper and regular with increasing feedback. The spatial power spectrum goes from multiple low-intensity peaks (at $\epsilon = 0$) to two isolated narrow peaks at high feedback. We compare theory and experiments by plotting the measured spatial bandwidth of the spectrum as a function of ϵ^2 [Fig. 1(b)]. The measured power spectrum is taken from the right column of Fig. 2. We took many more data points of different ϵ^2 values and from other regions of the crystal output, confirming that the behavior is always consistent with Figs. 1 and 2. The threshold behavior is clear in Fig. 2: the visibility of the stripes and the energy in the first spatial harmonic exhibit a clear jump at the threshold value. Comparing theory and experiments [Fig. 1(b)] shows much similarity [15]. At 6% feedback, a specific spatial frequency starts to dominate, and one can determine its bandwidth and plot it [Fig. 1(b)]. Increasing ϵ^2 further makes the bandwidth narrower with an increasing slope. The increasing negative slope in Fig. 1(b) between 0% and 15% feedback is a direct quantitative measure of the line narrowing of the stripes. When we increase ϵ^2 beyond 15%, we observe a clear inflection point in the graph, at which the second derivative of the bandwidth changes sign. This is the oscillation threshold. Increasing the feedback further results in more narrowing, but with a decreasing slope. The theoretical curve in Fig. 1(b) is calculated from Eq. (4) with the actual experimental parameters, adjusting only one parameter, ϕ_0, which cannot be measured independently. We measure the total intensity I and from it evaluate ψ_0 to be 53% of $\sqrt{I}$ via the best fit to our experiments.

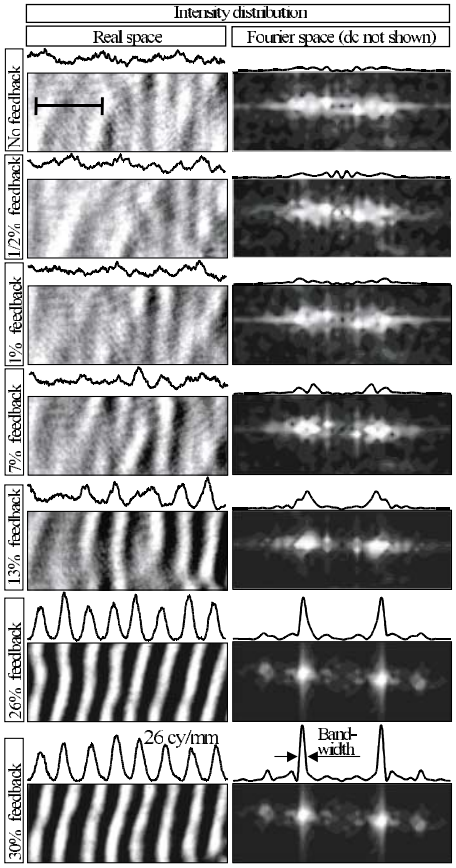

FIG. 2. Experimental results, bandwidth narrowing while increasing feedback. Shown are photographs of the intensity distribution in a specific region at the crystal output (left), along with the calculated spatial power spectrum (right). All measurements are taken without moving the crystal and without changing the nonlinearity. Bandwidth narrowing is obvious: the stripes become sharper and regular with increasing feedback, and the spatial power spectrum goes from multiple peaks (at no feedback) to two narrow peaks at high feedback.

Figure 1(b) proves that our theory truly describes the behavior of our system from zero feedback to the threshold. The threshold value, 14%, is beyond the $\epsilon \ll 1$ limit. In spite of that, our experiments agree well with the theory up to the threshold. Above threshold, we have no theory, but experimentally, we observe line narrowing down to the narrowest linewidth possible in our system. The characteristic behavior almost one-to-one resembles linewidth narrowing in lasers [7]. This is characteristic of systems undergoing a phase transition. We believe that other phase transition features occur in our system, with different characteristics than those of coherent cavities. For example, critical slowing down near the threshold should have different features from those in coherent cavities [16] and self-oscillators [17]. We emphasize that in our system the visibility of the pattern is always enhanced in the cavity as compared to MI without feedback under the same parameters. This is true even *below* threshold, in contrast to passive coherent cavities [2,4], where below threshold patterns are suppressed. Clearly, pattern formation in our cavity has different features than in a coherent cavity.

Let us discuss the differences between pattern formation in our cavity and in a single-mirror nonlinear

feedback system [4,18,19]. Most single-mirror systems rely on a fully coherent feedback, for which pattern formation is dominated by reflection gratings forming via interference between the input and feedback beams [19]. The difference between these cases and ours is obvious, as our cavity interference of beams from different cycles does not lead to an index grating. Some single-mirror systems do show patterns driven by incoherent feedback [18], which is seemingly similar to our cavity. Nevertheless, there are several major differences. For the single mirror, the spatial frequency of the pattern is fully determined by Talbot self-imaging (upon reflection from the mirror), which critically depends on the (small) spacing between the nonlinear sample and the mirror. This small spacing limits the range of spatial frequencies that can evolve. In our cavity, the cavity length is unimportant (as long as it is $\gg ct_c$), and there are no hard restrictions on the spatial frequencies, as we have a double $4f$ imaging system in the feedback. The spatial frequency of the pattern in our cavity depends only on Δn, the length of the nonlinear medium, and the Q factor of the cavity. Therefore, our cavity reveals fully the natural frequencies of the pattern arising from the MI, unaffected by bounday conditions. This is why we can study line narrowing of the natural spatial frequencies of the pattern. The single-mirror system is restricted by external boundary conditions, limiting the spatial frequencies that can evolve, whereas our cavity lets the spatial frequency of the highest nonlinear gain win.

In conclusion, we studied the evolution of patterns in a nonlinear cavity which is longer than the coherence length of the light circulating in it. The patterns exhibit spatial line narrowing as feedback is increased, resembling linewidth narrowing in lasers. This effect is characteristic of phase transitions, yet unlike other previously studied optical cavities, our cavity is incoherent. Our cavity relates to classical phase transitions, because its behavior does not depend on the phase, whereas pattern formation in coherent cavities is inherently phase dependent, thus related to nonclassical phase transitions. The distinctions between coherent and incoherent cavities and the parallels with lasers and phase transitions offer many exciting ideas. The ability to study pattern formation in systems of varying correlation has implications beyond optics; e.g., we envision partially incoherent cavities containing cooled atoms. We note the relation to patterns in granular materials (sand) [20], which displays the formation of stripes in a phase-independent system. In optics, however, the next idea is to study pattern formation in a fully incoherent cavity, that is, a cavity in which the circulating beam is spatially and temporally incoherent.

This work was supported by the Israeli Science Foundation and by the Ministry of Science, Israel.

[1] W.W. Rigrod, Appl. Phys. Lett. **2**, 51 (1963).
[2] F.T. Arecchi *et al.*, Phys. Rep. **318**, 1 (1999).
[3] S.R. Liu *et al.*, J. Opt. Soc. Am. B **9**, 1507 (1992); K. Staliunas *et al.*, Phys. Rev. A **51**, 4140 (1995); Phys. Rev. Lett. **79**, 2658 (1997); G.L. Oppo *et al.*, Phys. Rev. A **49**, 2028 (1994); S.J. Jensen *et al.*, Phys. Rev. Lett. **81**, 1614 (1998).
[4] W.J. Firth and A.J. Scroggie, Europhys. Lett. **26**, 521 (1994); Phys. Rev. Lett. **76**, 1623 (1996).
[5] M. Haelterman, S. Wabnitz, and S. Trillo, Opt. Lett. **17**, 745 (1992); S. Coen and M. Haelterman, Phys. Rev. Lett. **79**, 4139 (1997); Opt. Lett. **26**, 39 (2001).
[6] For cross-phase modulation in a cavity, two fields of orthogonal polarizations, each having its own resonant frequencies, interact through $\Delta n(I)$. In contrast to our case, for each polarization (separately) the interference between beams from different cycles critically contributes to Δn. See M. Haelterman *et al.*, J. Opt. Soc. Am. B **11**, 446 (1994).
[7] A. Yariv, *Quantum Electronics* (Wiley, New York, 1988), 3rd ed., p. 579.
[8] M. Soljacic *et al.*, Phys. Rev. Lett. **84**, 467 (2000); D. Kip *et al.*, Science **290**, 495 (2000).
[9] Going beyond lowest order analysis, the dominant modes are those of equal superposition of waves with q and $-q$, for which the visibility $|\psi_1|_{\max}/|\psi_0|$ is larger than that of nonequal superpositions.
[10] G. Agrawal, *Nonlinear Fiber Optics* (Academic Press, New York, 1995), p. 134.
[11] Near and above the threshold, our approximations fail. Relaxing $|\psi_1| \ll |\psi_0|$ adds "second-order MI," where higher harmonics of the dominant frequency considerably increase the visibility of the pattern—just as we observe experimentally. Including the contributions of beams that circulate more than once does not change the features but skews the threshold value.
[12] We examined the interference between the beams circulating in our cavity, at maximum feedback, and confirmed that there is no trace of interference between beams from different cycles even at detector integration times much shorter than τ.
[13] M. Segev *et al.*, Phys. Rev. Lett. **73**, 3211 (1994); D.N. Christodoulides *et al.*, J. Opt. Soc. Am. B **12**, 1628 (1995); M. Shih *et al.*, Electron. Lett.. **31**, 826 (1995).
[14] The MI pattern in our system consists of 1D stripes and not of 2D filaments even though our experiments are (2 + 1)D. The reason is twofold. First, the screening nonlinearity at low fields is higher in the direction of the bias; thus Δn is preferentially 1D. Second, the noise in most photorefractives comes from planar striations, also preferentially 1D. Thus, MI in photorefractives is 1D at low bias. Only at high fields (3 kV/cm), the space charge field is similar in both transverse directions, and the MI pattern contains hexagonic arrangements.
[15] Unit conversion is as in T. Carmon *et al.*, Phys. Rev. Lett. **87**, 143901 (2001).
[16] S. Ducci *et al.*, Phys. Rev. Lett. **83**, 5210 (1999).
[17] D. Engin *et al.*, Phys. Rev. Lett. **74**, 1743 (1995); S.G. Odoulov *et al.*, *ibid.* **83**, 3637 (1999).
[18] R. Macdonald *et al.*, Opt. Commun. **89**, 289 (1992).
[19] T. Honda, Opt. Lett. **18**, 598 (1993).
[20] O. Zik *et al.*, Phys. Rev. Lett. **73**, 644 (1994).